

Inclusive DIS at High Q^2 with Longitudinally Polarized Beams at HERA

JHEP 09 (2012) 061



Z. Zhang
LAL, Orsay

On behalf of
the H1 Collaboraton



HERA ep collider: largest electron microscope



HERA-1: 1992-2000, unpolarized beams

HERA-2: 2004-2007, longitudinally polarized e^\pm beams

Inclusive neutral current (NC) and charged current (CC) cross sections:

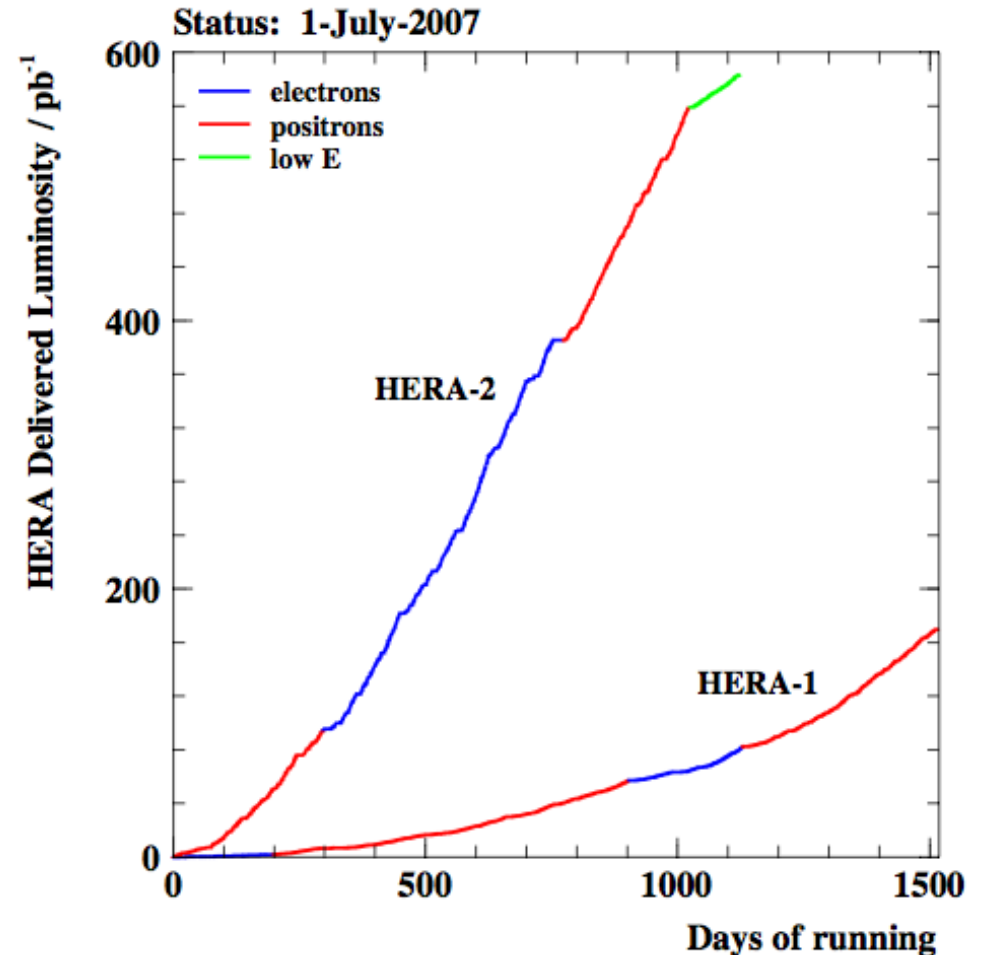
- Primary source for constraining Parton Distribution Functions (PDFs)
- Essential ingredients for making theoretical predictions at LHC

HERA-2 vs. HERA-1

4 distinct data sets at HERA-2:

| | <i>R</i> | <i>L</i> |
|--------|--|--|
| e^-p | $\mathcal{L} = 47.3 \text{ pb}^{-1}$ $P_e = (+36.0 \pm 1.0)\%$ | $\mathcal{L} = 104.4 \text{ pb}^{-1}$ $P_e = (-25.8 \pm 0.7)\%$ |
| e^+p | $\mathcal{L} = 101.3 \text{ pb}^{-1}$ $P_e = (+32.5 \pm 0.7)\%$ | $\mathcal{L} = 80.7 \text{ pb}^{-1}$ $P_e = (-37.0 \pm 0.7)\%$ |

Longitudinally polarized e^\pm beams at interaction point obtained from transversely polarized beams with spin rotators

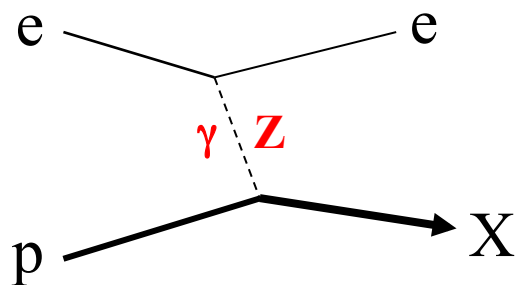


Lumi e^- ↗ ~10

Lumi e^+ ↗ ~3

Neutral and Charged Current DIS

NC e^+p event



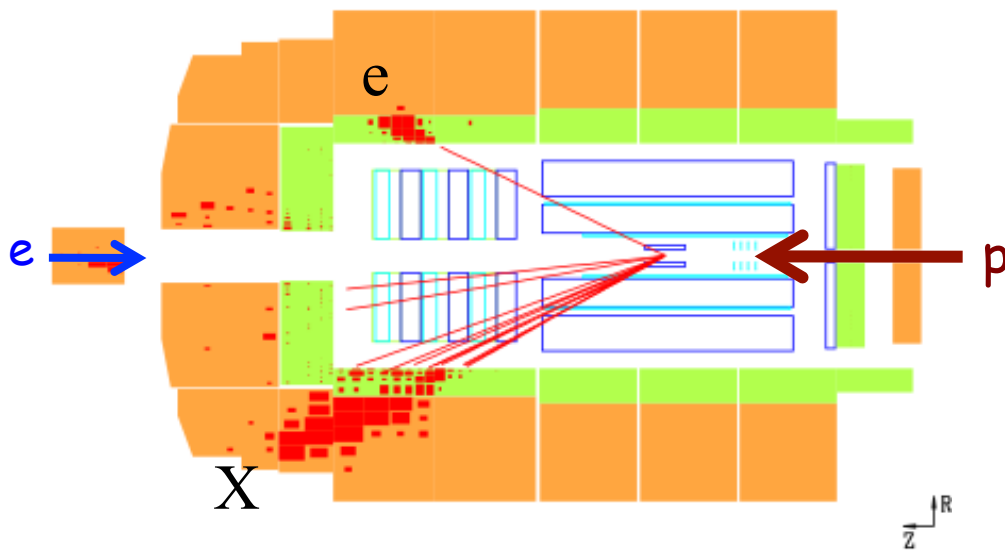
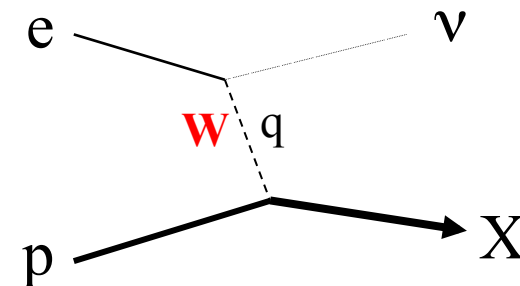
Event kinematics:

$$Q^2 = -q^2$$

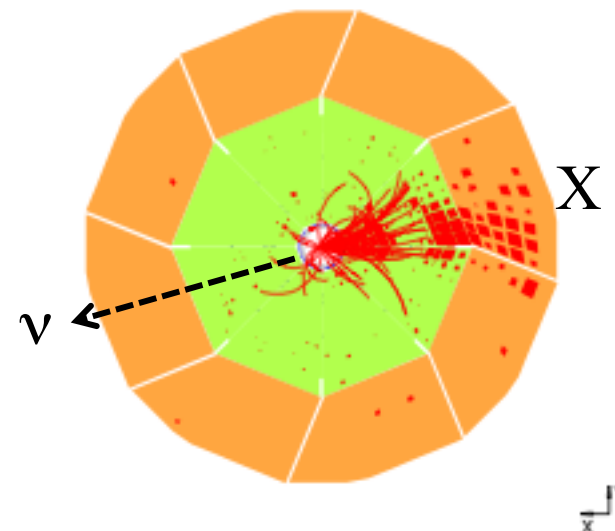
x : momentum fraction of struck parton

$y = Q^2/sx$: inelasticity

CC e^+p event



Final states e & X balanced in transverse plane



Unbalanced due to missing ν

Cross Sections, Structure Functions, PDFs

$$\frac{d^2\sigma_{\text{NC}}^{\pm}}{dx dQ^2} \sim Y_+ \tilde{F}_2 \mp Y_- x \tilde{F}_3^* \quad \text{with } Y_{\pm} = 1 \pm (1-y)^2$$

γ exchange

γZ interference

Z exchange

$$\tilde{F}_2 = F_2 - (\cancel{v_e} - P_e a_e) \kappa_Z F_2^{\gamma Z} + (\cancel{v_e}^2 + a_e^2 - \cancel{2P_e v_e a_e}) \kappa_Z^2 F_2^Z$$

$v_e \sim 0$, \rightarrow some of the terms are negligible

$$x \tilde{F}_3 = -(a_e - \cancel{P_e v_e}) \kappa_Z x F_3^{\gamma Z} + [2\cancel{v_e} a_e - P_e (\cancel{v_e}^2 + a_e^2)] \kappa_Z^2 x F_3^Z$$

$$\left[F_2, F_2^{\gamma Z}, F_2^Z \right] = x \sum_q \left[e_q^2, 2e_q v_q, v_q^2 + a_q^2 \right] \{ q + \bar{q} \}$$

$$\kappa_Z^{-1} = \frac{2\sqrt{2}\pi\alpha}{G_F M_Z^2} \frac{Q^2 + M_Z^2}{Q^2}$$

$$\left[x F_3^{\gamma Z}, x F_3^Z \right] = 2x \sum_q \left[e_q a_q, v_q a_q \right] \{ q - \bar{q} \}$$

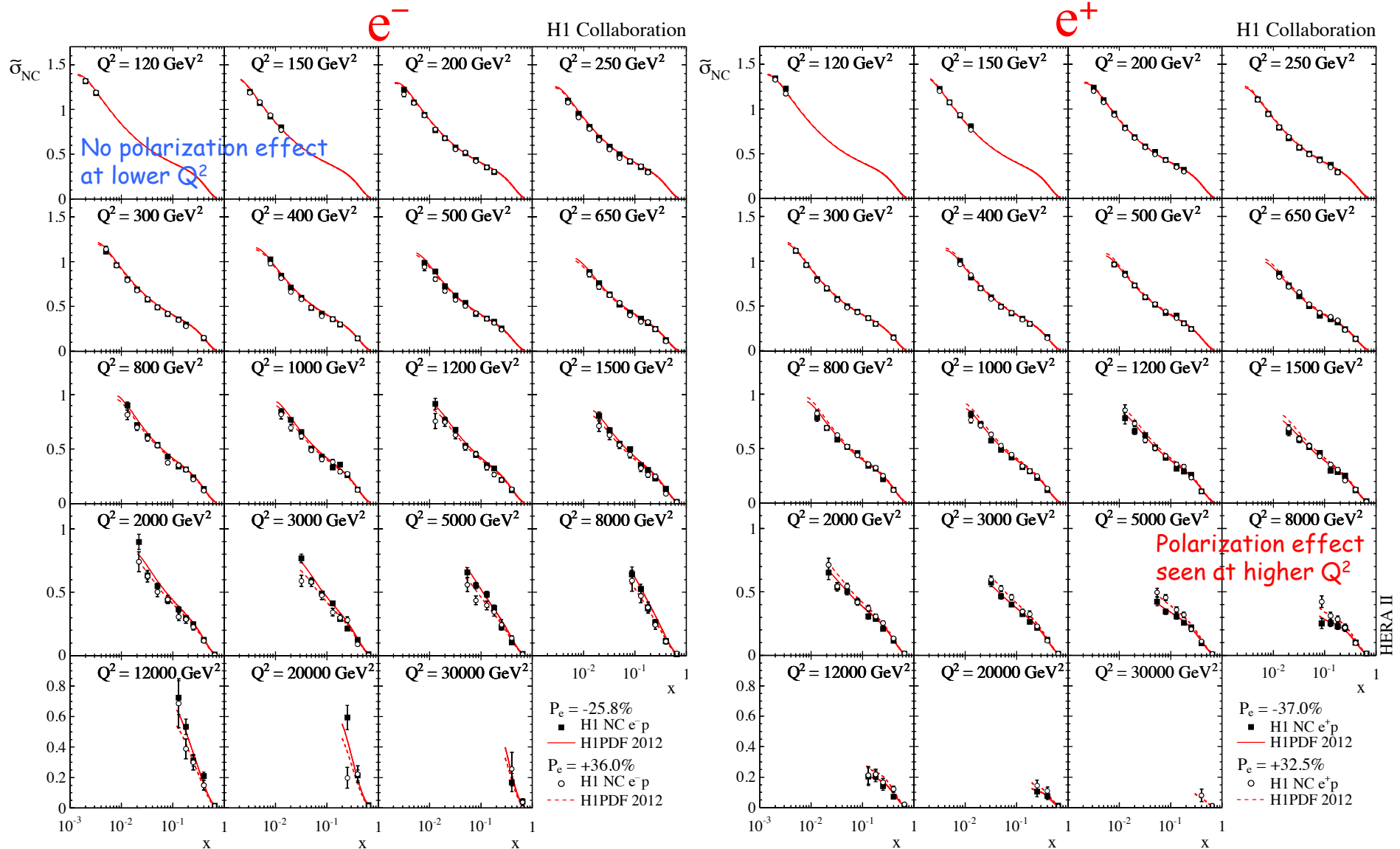
Structure function formulae given for e-p scattering, for e*p, $P_e \rightarrow -P_e$

CC cross sections have similar but different structure functions and PDF combinations

* $F_L=0$ in LO parton model,
 $F_L \sim g$ at NLO,
 Scaling violation $F_2 \rightarrow g$

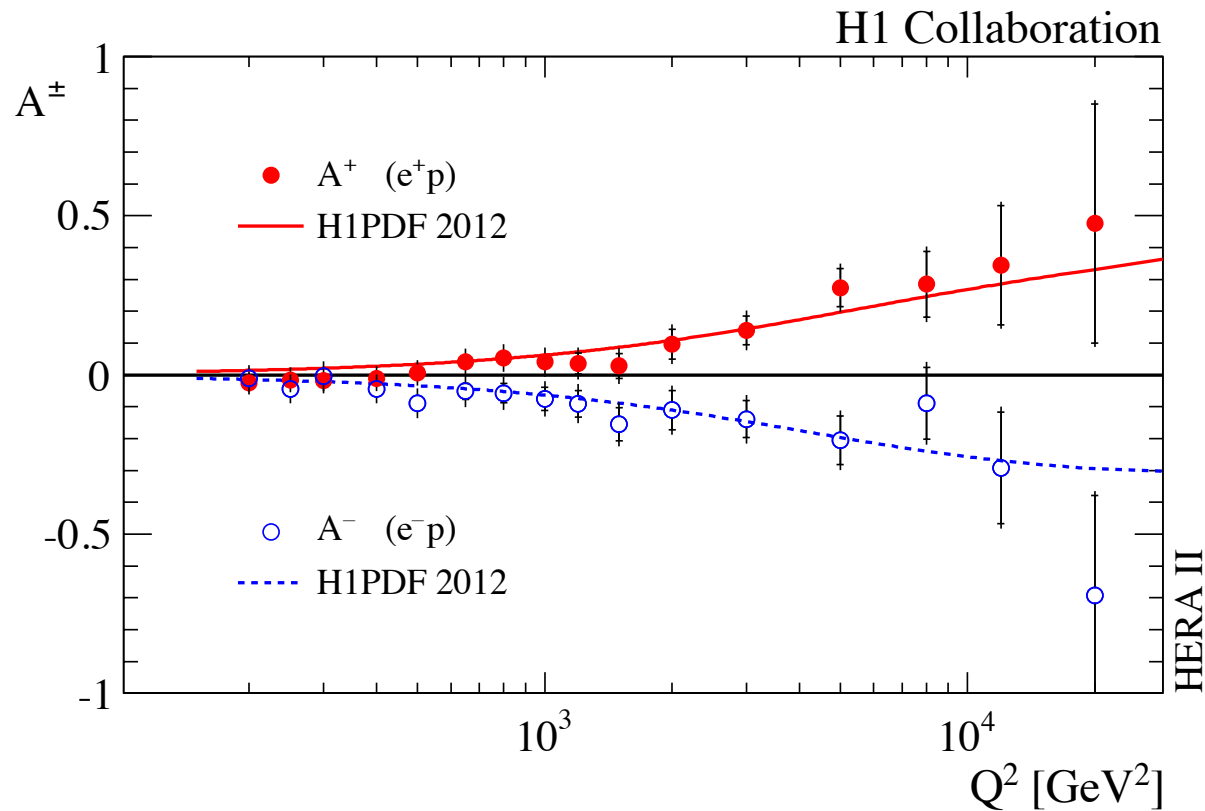
NC Double Differential Cross Sections

$$\tilde{\sigma}_{\text{NC}}^{\pm}(x, Q^2) \equiv \frac{d^2\sigma_{\text{NC}}^{\pm}}{dx dQ^2} \frac{xQ^4}{2\pi\alpha^2} \frac{1}{Y_{\pm}} = \left(\tilde{F}_2^{\pm} \mp \frac{Y_-}{Y_+} x\tilde{F}_3^{\pm} - \frac{y^2}{Y_+} \tilde{F}_L^{\pm} \right) (1 + \Delta_{\text{NC}}^{\text{weak}}) \quad Y_{\pm} = 1 \pm (1 - y)^2$$



NC Polarization Asymmetry

$$A^{\pm} = \frac{2}{P_L^{\pm} - P_R^{\pm}} \cdot \frac{\sigma^{\pm}(P_L^{\pm}) - \sigma^{\pm}(P_R^{\pm})}{\sigma^{\pm}(P_L^{\pm}) + \sigma^{\pm}(P_R^{\pm})}$$

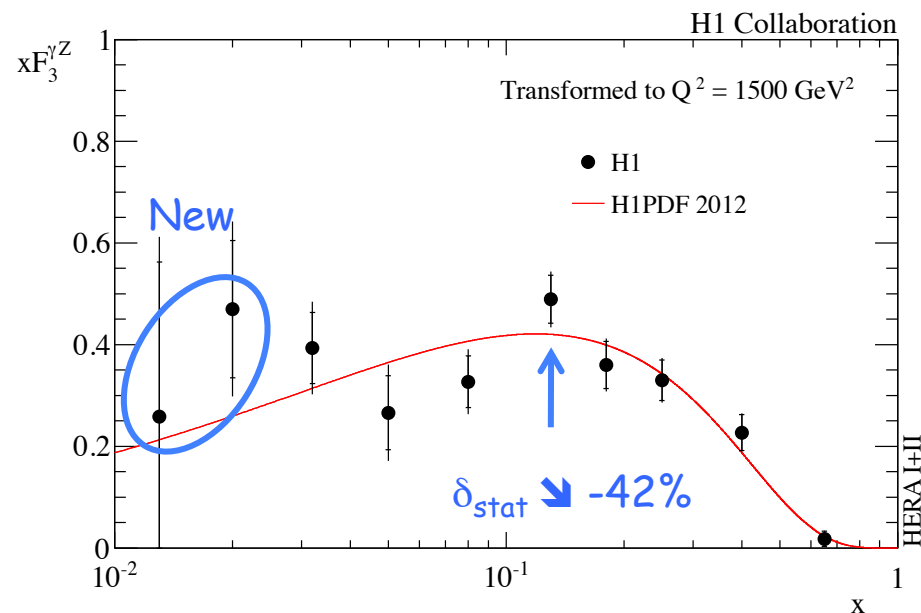
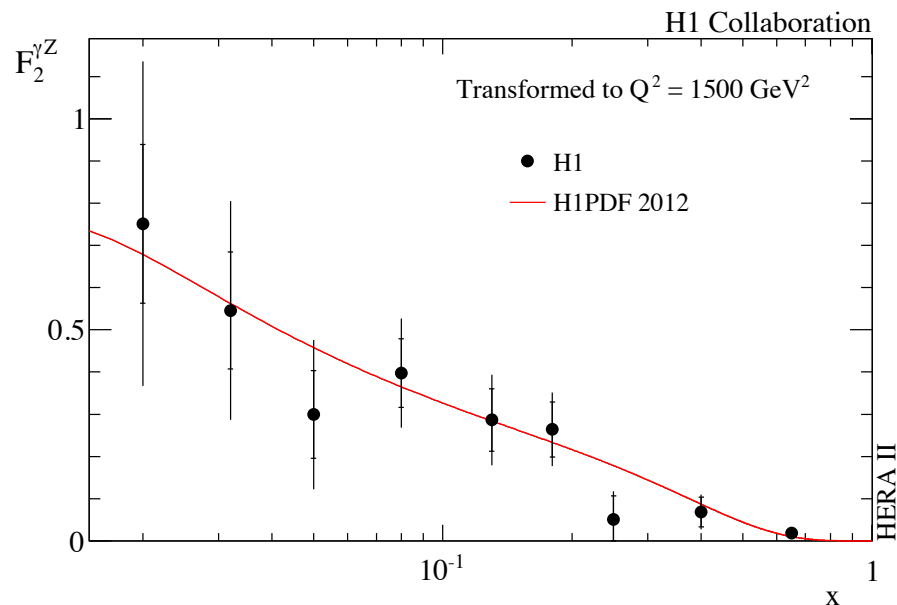


A direct measure of parity violation effect in NC DIS

Structure Functions $F_2^{\gamma Z}$, $xF_3^{\gamma Z}$

First measurement $F_2^{\gamma Z}$
extracted from polarized
NC cross sections

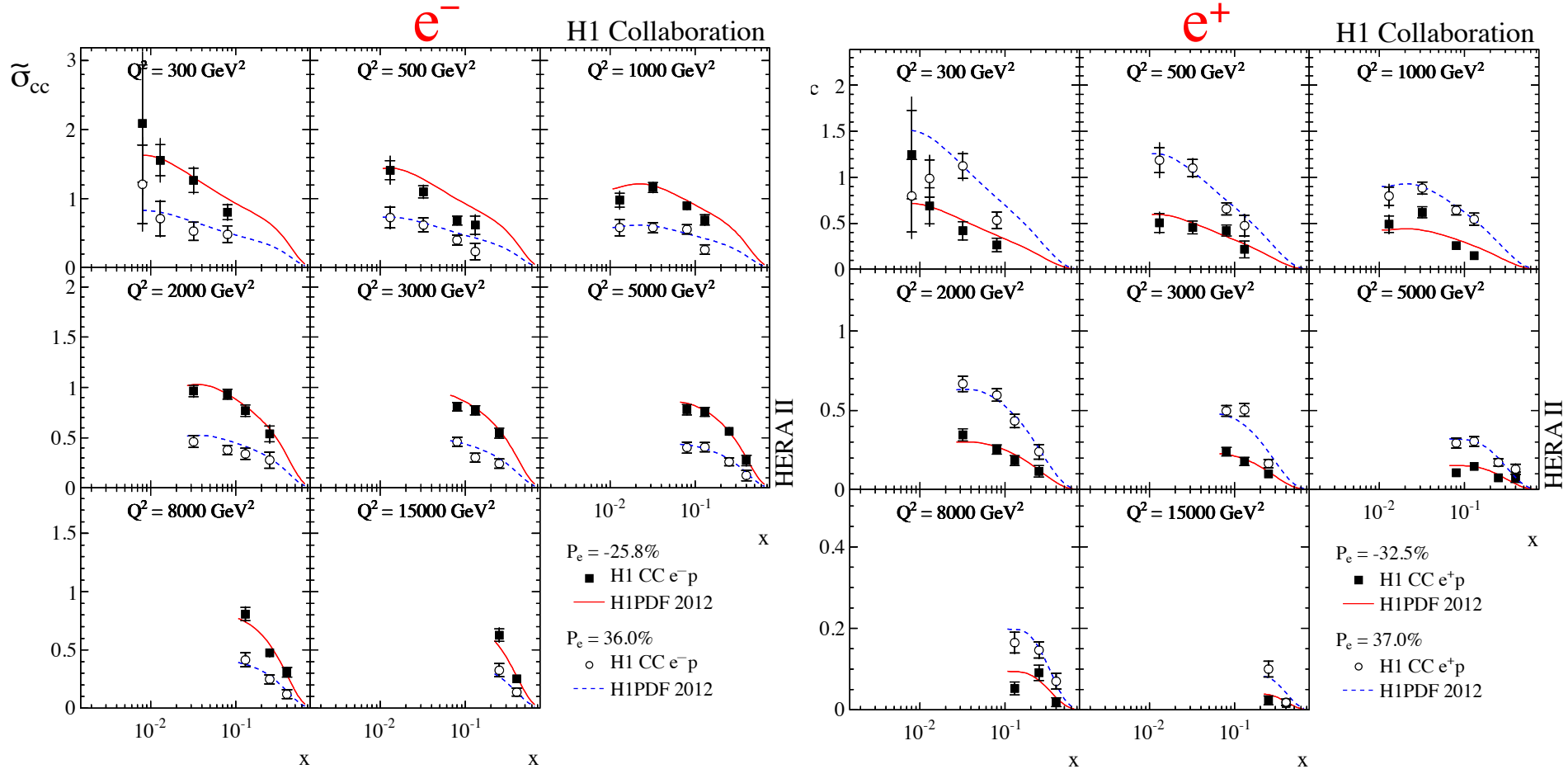
Improved $xF_3^{\gamma Z}$ using
combined HERA-1+2 data



x dependence of $F_2^{\gamma Z}$ and $xF_3^{\gamma Z}$ reflects their parton compositions
 $F_2^{\gamma Z} \sim q + \bar{q}$
 $xF_3^{\gamma Z} \sim xq_v$

CC Double Differential Cross Sections

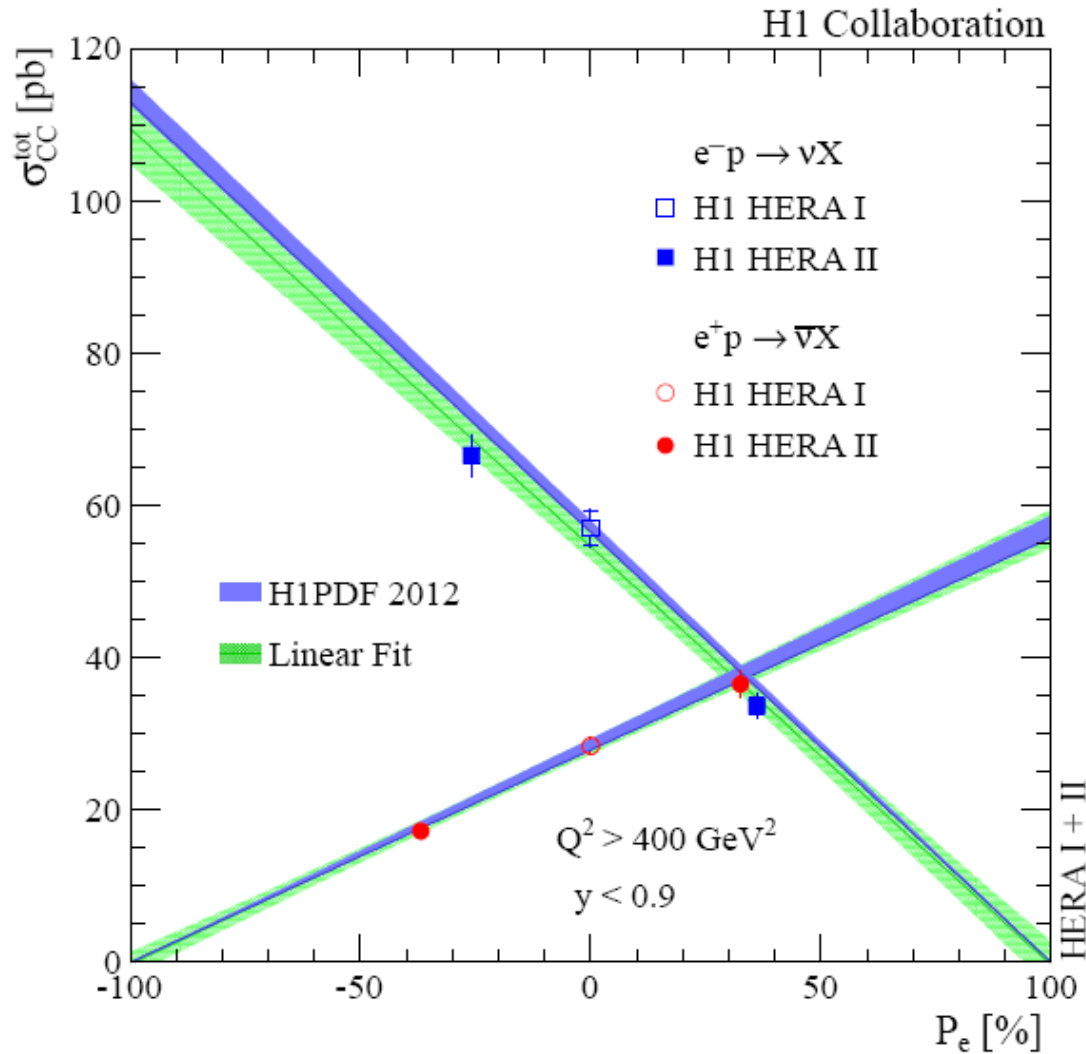
$$\tilde{\sigma}_{CC}^{\pm} \equiv \frac{4\pi x}{G_F^2} \left[\frac{M_W^2 + Q^2}{M_W^2} \right]^2 \frac{d^2\sigma_{CC}^{\pm}}{dx dQ^2} = (1 \pm P_e) (Y_+ W_2^{\pm} \mp Y_- x W_3^{\pm} - y^2 W_L^{\pm}) (1 + \Delta_{CC}^{\text{weak}})$$



CC cross sections have strong polarization dependence (P violation), provide unique flavor decomposition of proton

Total CC Cross Sections

SM CC: $\sigma_{CC}^{\pm}(P_e) = (1 \pm P_e)\sigma_{CC}^{\pm}(0)$

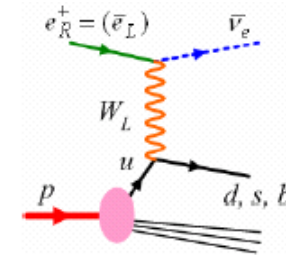


Right Handed CC: $\sigma_{RHCC}^{\pm}(P_e) = (1 \mp P_e)\sigma_{RHCC}^{\pm}(0)$

Extrapolated cross sections ~ 0

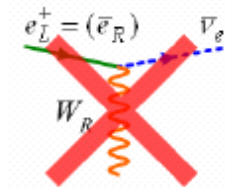
- at $P_e = +1$ for e^-
- at $P_e = -1$ for e^+

→ Only left-hand W in SM

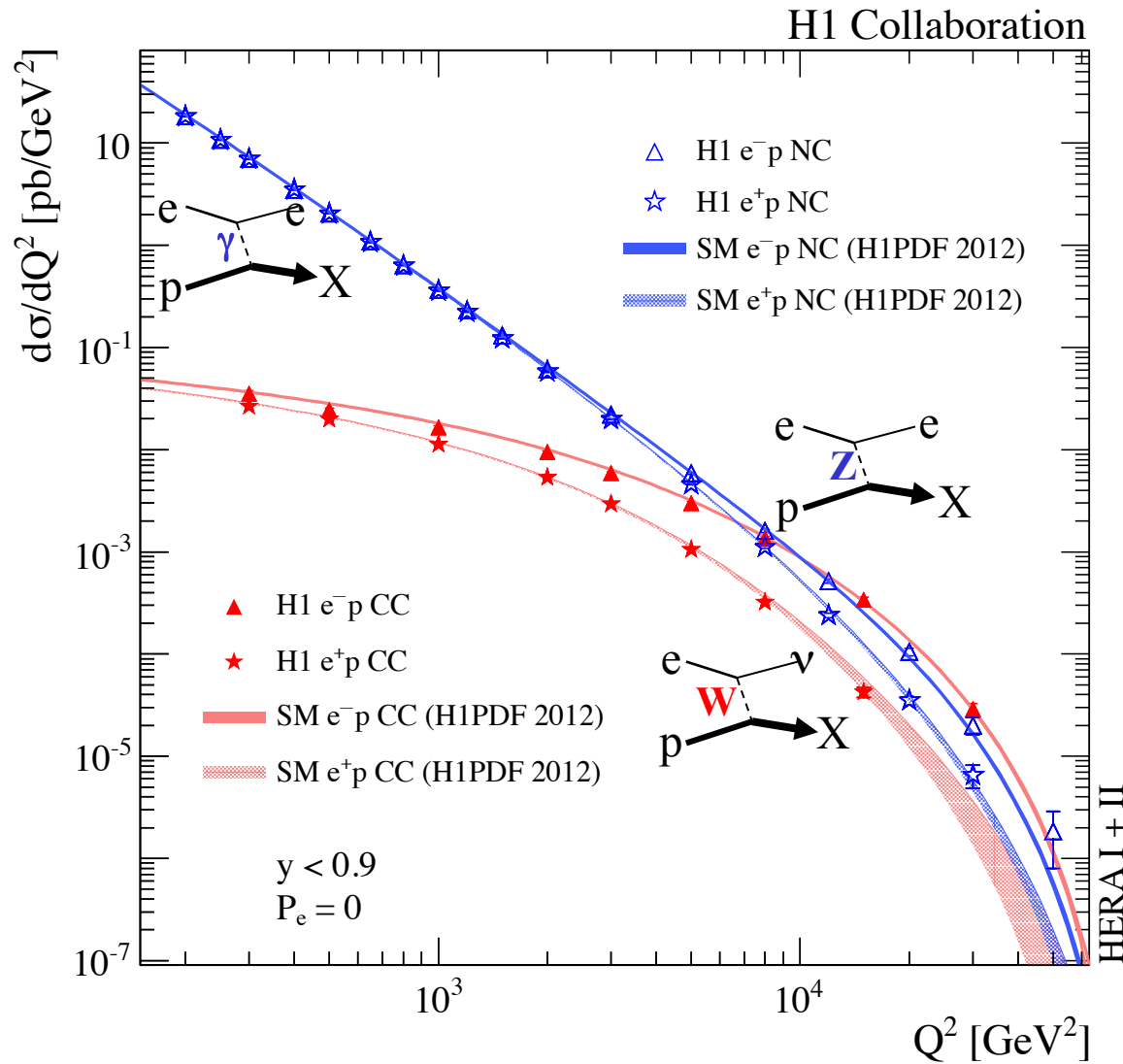


If $g_L = g_R$ & ν_R light

- e^- : $M_{WR} > 214 \text{ GeV}$ (95%CL)
- e^+ : $M_{WR} > 194 \text{ GeV}$ (95%CL)



HERA-1+2 Combined NC & CC $d\sigma/dQ^2$



Combined HERA-1+2 data

→ Typical total precision:

NC e^+ : ~1.5%

NC e^- : ~2.0%

CC e^\pm : ~4%

→ Beautiful illustration of unification of electromagnetic and weak interaction strength

New QCD Analysis: H1PDF 2012

In order to see the impact of the new HERA-2 NC+CC high Q^2 data on PDFs, a NLO QCD fit performed including all published H1 data

Published earlier HERA data have been the main inputs to all global PDFs fits

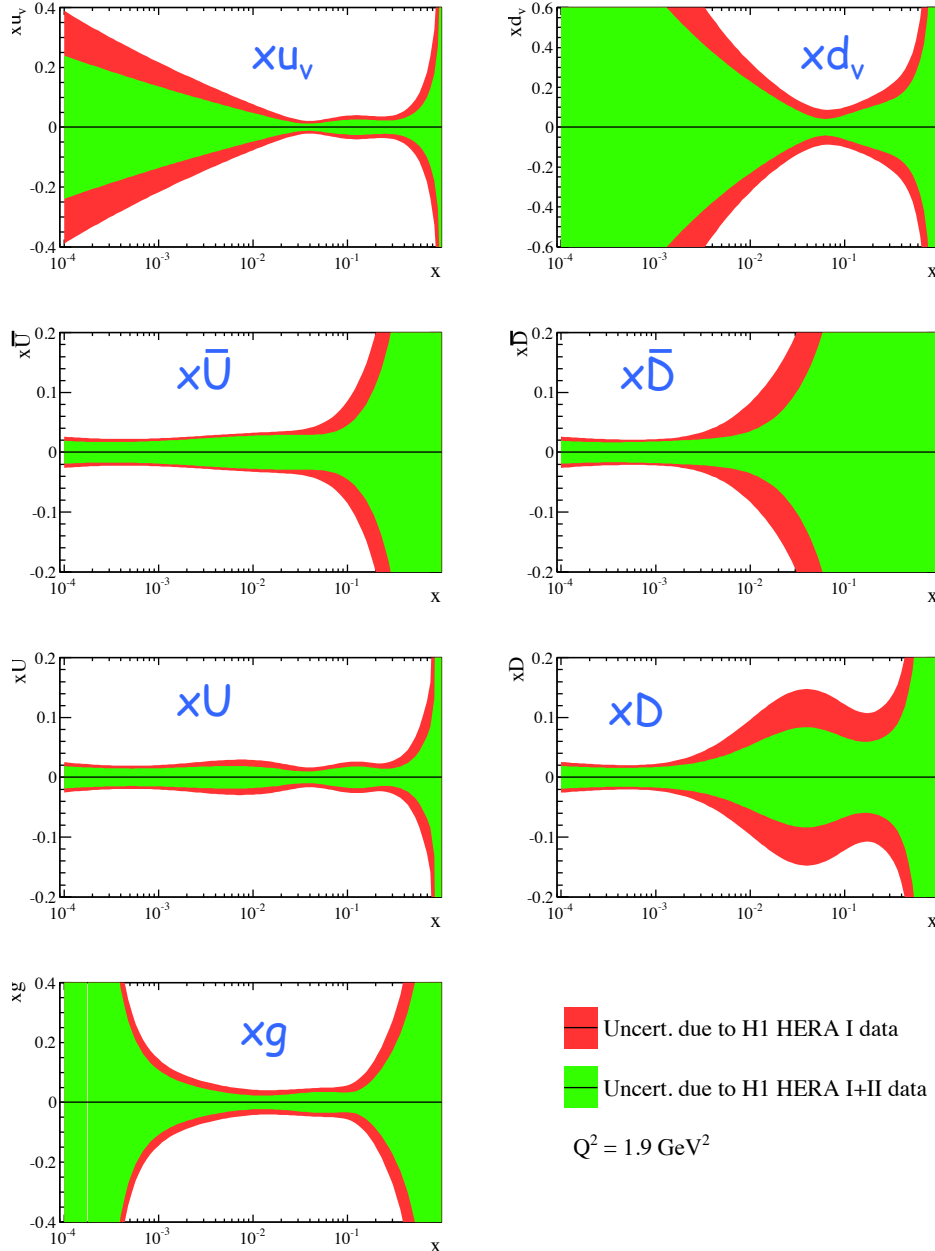
| Data set | x_{\min} | x_{\max} | Q_{\min}^2 (GeV ²) | Q_{\max}^2 (GeV ²) | $\delta\mathcal{L}$ (%) | Ref. | Comment |
|------------------------------|------------|------------|-------------------------------------|-------------------------------------|-----------------------------|------|---|
| e^+ Combined low Q^2 | 0.00004 | 0.20 | 0.5 | 150 | 0.5 | [72] | $\sqrt{s} = 301, 319$ GeV |
| e^+ Combined low E_p | 0.00003 | 0.003 | 1.5 | 90 | 0.5 | [72] | $\sqrt{s} = 225, 252$ GeV |
| e^+ NC 94-97 | 0.0032 | 0.65 | 150 | 30 000 | $0.5 \oplus 1.4$ | [1] | $\sqrt{s} = 301$ GeV |
| e^+ CC 94-97 | 0.013 | 0.40 | 300 | 15 000 | | | |
| e^- NC 98-99 | 0.0032 | 0.65 | 150 | 30 000 | | [2] | $\sqrt{s} = 319$ GeV |
| e^- CC 98-99 | 0.013 | 0.40 | 300 | 15 000 | $0.5 \oplus 1.7$ | | |
| e^- NC 98-99 <i>high y</i> | 0.00131 | 0.0105 | 100 | 800 | | | $\sqrt{s} = 319$ GeV |
| e^- NC 99-00 | 0.0032 | 0.65 | 150 | 30 000 | $0.5 \oplus 1.4$ | [3] | $\sqrt{s} = 319$ GeV; incl. <i>high y</i> |
| e^+ CC 99-00 | 0.013 | 0.40 | 300 | 15 000 | | | $\sqrt{s} = 319$ GeV |
| e^+ NC <i>high y</i> | 0.0008 | 0.0105 | 60 | 800 | $2.3 \oplus 1.0 \oplus 1.1$ | | $\sqrt{s} = 319$ GeV |
| e^- NC <i>high y</i> | 0.0008 | 0.0105 | 60 | 800 | $2.3 \oplus 1.2 \oplus 0.8$ | | $\sqrt{s} = 319$ GeV |
| e^+ NC <i>L</i> | 0.002 | 0.65 | 120 | 30 000 | $2.3 \oplus 1.5$ | | |
| e^+ CC <i>L</i> | 0.008 | 0.40 | 300 | 15 000 | | | $\sqrt{s} = 319$ GeV |
| e^+ NC <i>R</i> | 0.002 | 0.65 | 120 | 30 000 | $2.3 \oplus 1.5$ | | |
| e^+ CC <i>R</i> | 0.008 | 0.40 | 300 | 15 000 | | | |
| e^- NC <i>L</i> | 0.002 | 0.65 | 120 | 50 000 | $2.3 \oplus 1.5$ | | |
| e^- CC <i>L</i> | 0.008 | 0.40 | 300 | 30 000 | | | $\sqrt{s} = 319$ GeV |
| e^- NC <i>R</i> | 0.002 | 0.65 | 120 | 30 000 | $2.3 \oplus 1.5$ | | |
| e^- CC <i>R</i> | 0.008 | 0.40 | 300 | 15 000 | | | |

New

The data cover ~ 5 orders of magnitude in Q^2 and x

Impact of the New HERA-2 Data

H1 Collaboration



HERAFitter based on
QCDNUM (v17.04)
NLO, $\overline{\text{MS}}$ scheme
RT heavy flavor mass scheme

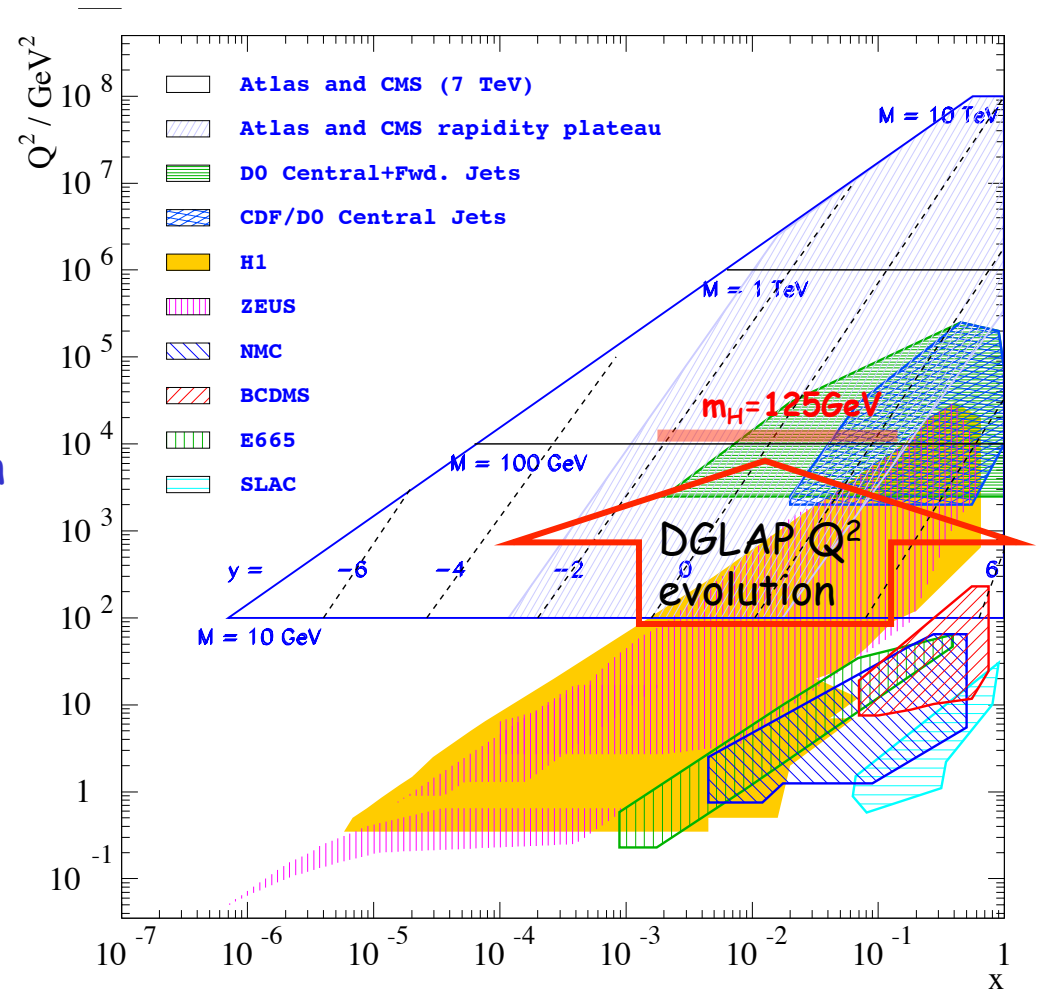
5 sets of PDFs with 13 free
parameters with quark number
and momentum sum rules:

$$\begin{aligned}
 xg(x) &= A_g x^{B_g} (1-x)^{C_g} - A'_g x^{B'_g} (1-x)^{25}, \\
 xu_v(x) &= A_{u_v} x^{B_{u_v}} (1-x)^{C_{u_v}} (1 + E_{u_v} x^2), \\
 xd_v(x) &= A_{d_v} x^{B_{d_v}} (1-x)^{C_{d_v}}, \\
 x\bar{U}(x) &= A_{\bar{U}} x^{B_{\bar{U}}} (1-x)^{C_{\bar{U}}}, \\
 x\bar{D}(x) &= A_{\bar{D}} x^{B_{\bar{D}}} (1-x)^{C_{\bar{D}}}.
 \end{aligned}$$

→ Improvement in precision
for all PDFs in full x range
in particular for down-type
quarks $x\bar{D}$

Summary

- With the polarized lepton beams at HERA-2, parity violation effects observed/confirmed with improved precision
- Absence of right-handed CC W boson
- First $F_2^{\gamma Z}$ and improved $x F_3^{\gamma Z}$ determinations
- NC & CC cross section data valuable for further constraining PDFs
- H1+ZEUS HERA-2 combination will come soon



The universal PDFs extracted from HERA can be directly applied to LHC in the relevant kinematic region through DGLAP Q^2 evolution